U.S. DEPARTMENT OF THE INTERIOR
U.S. GEOLOGICAL SURVEY

GEOLOGIC MAP OF SOUTH-CENTRAL YUCCA MOUNTAIN, NYE COUNTY, NEVADA

By

Robert P. Dickerson[1] and Ronald M. Drake II[2]

[1]S.M. Stoller Corp.

[2]U.S. Geological Survey

2004

Prepared in cooperation with the
YUCCA MOUNTAIN SITE CHARACTERIZATION OFFICE,
U.S. DEPARTMENT OF ENERGY, under
Interagency Agreement DE-AI08-02RW12167

Pamphlet to accompany
MISCELLANEOUS FIELD STUDIES MAP
MF–2422

CONTENTS

FIGURES

TABLE

CONVERSION FACTORS, VERTICAL DATUM, AND ABBREVIATIONS

Multiply	by	To obtain
millimeter (mm)	0.03937	inch (in.)
centimeter (cm)	0.3937	inch (in.)
meter (m)	3.281	foot (ft)
kilometer (km)	0.6214	mile (mi)

Sea level: In this report sea level refers to the National Geodetic Vertical Datum of 1929 (NVGD of 1929)—a geodetic datum derived from a general adjustment of the first-order-level nets of both the United States and Canada, formerly called Sea Level Datum of 1929.

The following terms and abbreviations also are used in this report:

ka	thousands of years before present
Ma	millions of years before present

DESCRIPTION OF MAP UNITS

QUATERNARY SURFICIAL DEPOSITS

Qac **Alluvial and colluvial deposits (Holocene)**—Grayish-tan to pale-brown to brown, poorly sorted silt, sand, gravel, and cobbles in alluvium and colluvium in and along active washes, as low floodplains above active channels, as vegetated bars, and as vegetated low-angle slopes; includes modern deposits on hill slopes; desert pavement absent to very poorly developed; no soil to very weak A/C soil development; matrix contains reworked, disseminated carbonate. Maximum thickness 54 m in borehole WT-10 (table 1)

Qc **Rock-fall, slope-failure, talus, and colluvial deposits (Holocene)**—Pale-brown to dark-brown, poorly sorted silt, sand, gravel, cobbles, and boulders in talus cones and talus deposits on steep-sided hills and at base of small cliffs; characteristically forms "rock stripes" of talus typically exhibiting well-developed desert varnish; includes debris weathered from bedrock on steep slopes and debris flows localized in steep gullies; deposits lack desert pavement development or soil development, although locally cemented with caliche; matrix contains reworked, disseminated carbonate. Maximum thickness likely less than 4 m

MIOCENE VOLCANIC ROCKS

Timber Mountain Group

mrw **Rainier Mesa Tuff, welded**—Light-gray to pinkish-gray, devitrified, partly to moderately welded, rhyolitic ash-flow tuff. Contains 10–20 percent phenocrysts of quartz, sanidine, plagioclase, and biotite; 8–20 percent pumice, 0.3–10 cm in diameter; and as much as 2 percent dark-gray to dark-brown lithic fragments of devitrified volcanic rock. Exposures limited to eastern and western edges of map area. Unit boundaries from Day, Dickerson, and others (1998). Maximum thickness 27 m

mr **Rainier Mesa Tuff, nonwelded to partly welded**—Light-gray to light-tan, partly vitric to devitrified, nonwelded to partly welded, rhyolitic ash-flow tuff. Contains 12–20 percent phenocrysts of quartz, sanidine, plagioclase, and biotite; 8–20 percent vitric pumice, 0.3–10 cm in diameter; and as much as 2 percent dark-gray to dark-brown lithic fragments of devitrified volcanic rock. Basal part of unit is bedded tuff grading upward into massive nonwelded tuff. Unit boundaries from Day, Dickerson, and others (1998). Maximum thickness 145 m

Paintbrush Group

bt5 **Bedded tuff**—White to buff, devitrified, nonwelded bedded tuff. Contains as much as 30 percent white to light-gray pumice and altered pumice; and 5–8 percent light-brown to grayish-red lithic fragments. Locally includes pyroclastic flow and fallout deposits. Limited exposures in southeast corner and south-central part of map area. Unit boundaries from Day, Dickerson, and others (1998). Maximum thickness 4.6 m

px **Paintbrush Group, undivided tectonic fault slivers and breccia**—Tectonically juxtaposed blocks and highly brecciated material consisting of welded tuff from various zones and subzones within the Tiva Canyon Tuff and the Topopah Spring Tuff. Exposed predominantly in hanging-wall deformation zones associated with block-bounding Solitario Canyon fault zone. Limited exposures in northwest corner and east-central and southeastern parts of map area. Unit boundaries from Day, Dickerson, and others (1998)

Tiva Canyon Tuff

Crystal-rich member

cr **Crystal-rich member, undivided**—Pale-brown to brownish-black to pinkish-gray, predominantly devitrified, moderately to densely welded, quartz latitic ash-flow tuff. Contains 7–15 percent phenocrysts of sanidine, plagioclase, biotite, and traces of hornblende, sphene, and pyroxene; 1–20 percent light- to dark-gray and reddish-brown, moderately to slightly deformed pumice, 1–3 cm in

diameter; and sparse light-gray to dark-reddish-gray to brown lithic fragments, 1–10 mm in diameter. Lithophysae (locally as much as 20 percent) common within unit; lithophysae typically equant and as much as 20 cm in diameter. Unit typically forms a ledge and cap rock to the Tiva Canyon Tuff. Only shown in eastern and western parts of map area based on 1:24,000-scale data (Day, Dickerson, and others, 1998)

cr4 **Vitric and subvitric transition zone**—Pale-reddish-brown to brownish-black, vitric to partly devitrified, densely to partly welded, quartz latitic ash-flow tuff. Contains as much as 15 percent phenocrysts of sanidine, plagioclase, biotite, and traces of hornblende, sphene, and pyroxene; and 5–15 percent white to light-gray to yellowish-brown pumice, 1–3 cm in diameter. Unit locally includes following units of Buesch and others (1996): crystal-rich subvitrophyre transition subzone, densely welded interval (Tpcrn4d); crystal-rich nonlithophysal subvitrophyre transition subzone, moderately welded interval (Tpcrn4m); and crystal-rich vitric moderately welded subzone (Tpcrv2). Unit occurs in tectonic slivers of fault zones and in southeastern part of map area near Dune Wash. Maximum thickness approximately 3 m

cr3 **Pumice-poor zone**—Reddish-brown to light-brownish-gray to pale-brown, devitrified, moderately to densely welded, nonlithophysae-bearing, quartz latitic ash-flow tuff. Contains 12–15 percent phenocrysts of sanidine, plagioclase, biotite, and trace of hornblende, sphene, and pyroxene; 1–5 percent light-gray and yellowish-brown to pale-reddish-brown pumice and altered pumice; and less than 1 percent lithic fragments. Unit correlative to crystal-rich nonlithophysal pumice-poor subzone (Tpcrn3) of Buesch and others (1996). Occurs in down-dropped fault blocks in Dune Wash and along the Abandoned Wash fault. Thickness 1.5–3 m

cr2 **Mixed pumice zone**—Light-gray to light-brownish-gray, moderately to densely welded, devitrified, quartz latitic ash-flow tuff. Contains 10–15 percent phenocrysts of sanidine, plagioclase, biotite, and trace of hornblende, sphene, and pyroxene; abundant (as much as 20 percent) light- to dark-gray and reddish-brown, moderately to slightly deformed pumice, 1–15 cm in diameter; and sparse light-gray to dark-reddish-gray to brown lithic fragments. Lithophysae (locally as much as 20 percent) common throughout unit; lithophysae typically equant and as much as 20 cm in diameter. Unit locally includes crystal-rich nonlithophysal mixed pumice subzone (Tpcrn2) of Buesch and others (1996). Contact with subjacent unit is transitional over a vertical distance of 1 m. Unit forms bench at top of the Tiva Canyon Tuff. Thickness 8–15 m

cr1 **Transition zone**—Light-gray to light-brownish-gray, densely welded, devitrified, quartz latitic ash-flow tuff. Contains 7–10 percent phenocrysts of sanidine, plagioclase, biotite, and trace of hornblende, sphene, and pyroxene; approximately 5 percent light-gray and light-yellowish-gray altered pumice; and sparse light-gray to dark-reddish-gray to brown lithic fragments. Commonly as much as 15 percent lithophysal cavities; lithophysae are equant and as much as 20 cm in diameter. Unit locally includes following units of Buesch and others (1996): crystal-rich transition lithophysal subzone (Tpcrl1); and crystal-rich transition nonlithophysal subzone (Tpcrn1). Contact with subjacent zone is transitional over a vertical distance of 1.5 m. Unit forms smooth, rounded outcrops at or below base of small step at top of the Tiva Canyon Tuff. Unit is very tough, and produces rock shrapnel when struck with a hammer. Thickness 4.5–9 m

Crystal-poor member

cp **Crystal-poor member, undivided**—Light-gray to brownish-gray to pinkish-gray to grayish-red to dark-gray, predominantly devitrified, moderately to densely welded, rhyolitic ash-flow tuff. Contains 3–7 percent phenocrysts of sanidine, plagioclase, and rare biotite and altered hornblende; 0–20 percent light- to dark-gray, slightly to intensely deformed pumice; and sparse light-gray to dark-reddish-gray lithic fragments, 1–10 mm in diameter. Lithophysae (locally as much as 20 percent) common within unit in distinct zones; lithophysae typically equant

and irregularly shaped in upper part of unit, and oblate in lower part of unit. Unit typically forms a slope locally covered by dark-colored loose rock. Only shown in eastern and western parts of map area based on 1:24,000-scale data (Day, Dickerson, and others, 1998)

cpul **Upper lithophysal zone**—Light-gray to pinkish-gray, densely welded, devitrified, rhyolitic ash-flow tuff. Contains approximately 7 percent phenocrysts of sanidine, plagioclase, and trace of biotite and altered hornblende and pyroxene; 0–5 percent highly altered light-gray pumice; sparse pale-brownish-pink lithic fragments, less than 1 cm in diameter; 5–20 percent lithophysae, 2–10 cm in diameter, size decreasing downward. Lithophysae commonly exhibit a 1- to 5-mm-thick vapor-phase alteration rind. Contact with subjacent zone is transitional over a vertical distance of 1 m. Unit forms slopes below step at top of the Tiva Canyon Tuff. Unit breaks much more easily than overlying crystal-rich transition zone (cr1). Thickness 0–21 m

cpun **Upper nonlithophysal zone**—Light-gray to light-brownish-gray, densely welded, devitrified, rhyolitic ash-flow tuff. Contains 4–6 percent phenocrysts of sanidine, plagioclase, and rare biotite and altered hornblende; 0–5 percent gray pumice; and sparse light-gray lithic fragments, less than 1 cm in diameter. Unit forms a mappable nonlithophysal zone correlative with upper nonlithophysal subzone (Tpcpmn3) of Buesch and others (1996). Contact with subjacent zone is transitional over a vertical distance of 1–2 m. Lower contact is defined at upper limit of large, irregular lithophysae. Unit characterized by easy breakage with conchoidal fracture, and distinctive ring when struck with hammer. Forms slopes characteristically covered by dark-colored, loose, angular rock. Thickness 0–12 m

cpml **Middle lithophysal zone**—Light-gray to light-brownish-gray, densely welded, devitrified, rhyolitic ash-flow tuff. Contains 3–5 percent phenocrysts of sanidine, plagioclase, and rare biotite and altered hornblende; 0–2 percent gray pumice; and sparse light-gray lithic fragments, less than 1 cm in diameter. Contains 2–8 percent lithophysae that range from 2–4 cm in diameter and oblate in shape, to 6–10 cm in diameter and irregular in shape. Unit forms mappable zone correlative with middle lithophysae-bearing subzone (Tpcpmn2) of Buesch and others (1996). Contact with subjacent zone is transitional over a vertical distance of 1–2 m, and includes vapor-phase partings. Unit characterized by easy breakage with conchoidal fracture, and distinctive ring when struck with hammer. Locally forms slopes characteristically covered by dark-colored, loose, angular rock. Thickness 0–15 m

cpmn **Middle nonlithophysal zone**—Light-gray to light-brownish-gray to pale-red, densely welded, devitrified, rhyolitic ash-flow tuff. Contains 3–6 percent phenocrysts of sanidine, plagioclase, and rare biotite and altered hornblende; 0–5 percent gray pumice; and sparse light-gray lithic fragments less than 1 cm in diameter. Locally contains sparse lithophysae, 2–4 cm in diameter, in lower part of unit. Unit locally includes following units of Buesch and others (1996): upper nonlithophysal subzone (Tpcpmn3), middle lithophysae-bearing subzone (Tpcpmn2), and lower nonlithophysal subzone (Tpcpmn1). Contact with subjacent zone is transitional over a vertical distance of 1–2 m, and includes vapor-phase partings. Locally, lower contact lies just below an angular bench that separates hackly fractured rock below from conchoidally fractured rock above. Unit characterized by easy breakage with conchoidal fracture, and distinctive ring when struck with hammer. Forms slopes characteristically covered by dark-colored, loose rock. Thickness 12–45 m

cpll **Lower lithophysal zone**—Pale-red to grayish-red to light-brownish-gray, densely welded, devitrified, rhyolitic ash-flow tuff. Contains 2–3 percent phenocrysts of sanidine, plagioclase, and rare altered hornblende; 0–5 percent devitrified gray pumice; less than 2 percent light-gray lithic fragments, less than 1 cm in diameter; 2–20 percent oblate lithophysae, less than 5 cm in diameter; and lesser amounts of vapor-phase partings in uppermost and lowermost part of zone. Lithophysae commonly exhibit a vapor-phase alteration rind about 5 mm thick.

Hackly fracturing characteristic of lower part. Contact with subjacent zone is transitional over a vertical distance of 1–2 m. Slope-forming unit within map area; locally forms a rounded step. Thickness 6–21 m

cpln **Lower nonlithophysal zone**—Pale-red to grayish-red to light-gray to dark-gray, moderately to densely welded, devitrified, rhyolitic ash-flow tuff. Contains 2–3 percent phenocrysts of sanidine, plagioclase, and rare altered hornblende; 0–15 percent dark-gray, devitrified, flattened pumice and black, vitric, flattened pumice, 2–6 cm long; less than 1 percent dark-reddish-gray lithic fragments, less than 1 cm in diameter. Contains oblate cavities that exhibit internal spherulites; these cavities are casts of weathered-out pumice clasts. Unit contains vapor-phase partings in very uppermost part. Unit exhibits a hackly fracture that extends upward into overlying unit cpll and is not particularly unique to either unit. Unit locally may exhibit poorly developed subvertical columnar cooling joints in lower part. Where unit cplnc is present, contact with subjacent unit is fairly sharp; where unit cplnc is absent, contact is transitional over a vertical distance of less than 1 m. Unit usually forms a slope but locally forms a small cliff. Thickness 6–40 m

cplnc ***Columnar subzone***—Lithologically similar to unit cpln, but characterized by prominent subvertical columnar cooling joints. Locally, lowest part is partly vitric. Unit typically forms a small cliff or step at base of unit cpln, and locally may form two steps. Thickness 0–9 m

cpv **Vitric zone**—Light-orangish-brown to light-gray, partly welded, vitric, rhyolitic ash-flow tuff. Contains 2 percent phenocrysts of sanidine and plagioclase; 2–15 percent (locally as much as 25 percent) vitric, partly flattened to undeformed pumice; and 0–5 percent dark-reddish-gray volcanic lithic clasts less than 2 cm in diameter. Unit usually includes nonwelded to partially welded subzone (Tpcpv1) of Buesch and others (1996), but locally includes moderately welded subzone (Tpcpv2) and densely welded subzone (Tpcpv3), which is present as basal vitrophyre. Contact with subjacent unit is sharp. Unit forms a distinctive orange-colored slope and small bench, and locally forms black, cliff-forming vitrophyre. Thickness 2.7–11 m

bt **Pre-Pah Canyon bedded tuff**—White, light-gray, pale-orange, and light-brown, nonwelded, vitric to devitrified rhyolitic fallout tephra and ash-flow tuff. Contains 2–10 percent phenocrysts of sanidine, plagioclase, and trace of biotite, pyroxene, and magnetite; 2–15 percent gray, reddish-gray, and brown devitrified rhyolite and grayish-black obsidian lithic fragments; and 15–85 percent white, light-gray, pink, light-to-moderate-brown, and light-green vitric to devitrified and altered pumice, 5–25 mm in diameter. Unit includes pre-Tiva Canyon bedded tuffs (bedded tuff 4 units A and B) of Moyer and others (1996), pre-Yucca Mountain nonwelded bedded tuff (bedded tuff 3) of Moyer and others (1996), pre-Pah Canyon nonwelded bedded tuff (bedded tuff 2) of Moyer and others (1996), distal facies of the Pah Canyon Tuff, and crystal-rich vitric nonwelded subzone of the Topopah Spring Tuff (Tptrv3) of Buesch and others (1996). Unit forms a light-colored gentle slope. Thickness 8–20 m

Topopah Spring Tuff

Crystal-rich member

tx **Undivided tectonic fault slivers and breccia**—Tectonically juxtaposed blocks and highly brecciated material consisting of welded tuff from various zones and subzones within the Topopah Spring Tuff. Exposed predominantly in hanging-wall deformation zones. Limited exposures in northwestern and southeastern corners of map area based on 1:24,000-scale data from Day, Dickerson, and others (1998)

tr **Vitric and densely welded zones and nonlithophysal zone, undivided**—Includes vitric zone and densely welded zone, undivided (unit trv) and nonlithophysal zone (unit trn) of crystal-rich member of the Topopah Spring Tuff. Mapped where unit trv is present but poorly exposed as on Bow Ridge. Limited exposures in northeast corner of map area based on 1:24,000-scale data from Day, Dickerson, and others (1998)

trv **Vitric zone and densely welded zone, undivided**—Dark-reddish-brown to dark-red, densely welded, vitric to partly devitrified, quartz latitic ash-flow tuff. Contains 10–15 percent phenocrysts of sanidine, plagioclase, biotite, and trace of clinopyroxene and hornblende; 2–10 percent pumice; and sparse lithic fragments. Unit locally includes following units of Buesch and others (1996): crystal-rich densely welded vitrophyre interval (Tptrv1v) and crystal-rich vitric moderately welded subzone (Tptrv2). Forms ledge at top of cliff at top of the Topopah Spring Tuff. Thickness 2.7–8 m

trn **Nonlithophysal zone**—Grayish-brown to pale-red-brown to light-brown, densely welded, devitrified, pumice-rich, quartz latitic ash-flow tuff. Contains 10–15 percent phenocrysts of sanidine, plagioclase, biotite, and trace of clinopyroxene and hornblende; 10–25 percent mixed light (white to light gray) and dark (reddish gray to dark gray) pumice; and minor lithic fragments. Characterized by abundant vapor-phase corrosion of pumice. Unit locally includes following units of Buesch and others (1996): crystal-rich nonlithophysal dense subzone (Tptrn3), crystal-rich nonlithophysal vapor-phase corroded subzone (Tptrn2), and crystal-rich transition nonlithophysal subzone (Tptrn1). Forms prominent cliff at top of the Topopah Spring Tuff. Thickness 19–35 m

trl **Lithophysal zone**—Reddish-brown to light-brown, densely welded, devitrified, quartz latitic ash-flow tuff. Contains 10–15 percent phenocrysts of sanidine, plagioclase, biotite, and trace of clinopyroxene and hornblende; as much as 10 percent mixed light (white to light gray) and dark (reddish gray to dark gray) pumice; and minor lithic fragments. Characterized by abundant lithophysae, 1–3 cm in diameter. Unit locally includes following units of Buesch and others (1996): crystal-rich lithophysal subzone (Tptrl2) and crystal transition lithophysal subzone (Tptrl1). Forms an irregular, rocky rib west of Dune Wash. Thickness 0–5 m

Crystal-poor member

tpul **Upper lithophysal zone**—Light-gray to light- to moderate-brown and pale-red-purple, densely welded, devitrified, rhyolitic ash-flow tuff. Contains 2–5 percent phenocrysts of sanidine, plagioclase, and minor biotite; and 0–10 percent devitrified pumice. Characterized by 5–30 percent equant lithophysae, from 1 to more than 10 cm in diameter. Lithophysae typically have 1- to 5-mm-thick vapor-phase alteration rind. Unit includes following units of Buesch and others (1996): crystal-poor upper lithophysal zone (Tptpul) and crystal-poor cavernous lithophysal subzone (Tptpulc). Upper part of unit may form lowest part of prominent cliff at top of the Topopah Spring Tuff but most of unit forms a slope below cliff. Thickness 41–61 m

tpmn **Middle nonlithophysal zone**—Grayish-orange-pink and light-brown to light-gray, densely welded, devitrified, rhyolitic ash-flow tuff. Contains 1–2 percent phenocrysts of sanidine, plagioclase, and minor biotite; and 0–3 percent devitrified pumice, 1–10 mm in diameter. Locally contains some equant lithophysae. Lithophysae typically have 1- to 5-mm-thick vapor-phase alteration rind. Unit includes following units of Buesch and others (1996): crystal-poor middle nonlithophysal zone (Tptpmn), upper nonlithophysal subzone (Tptpmn3), lithophysae-bearing subzone (Tptpmn2), and lower nonlithophysal subzone (Tptpmn1) of middle nonlithophysal zone. Unit forms slope below prominent cliff at top of the Topopah Spring Tuff. Thickness 43–47 m

tpll **Lower lithophysal zone**—Shown in cross sections only. Pale-red, grayish-red-purple, and light-brown, densely welded, devitrified, rhyolitic ash-flow tuff. Contains 1–2 percent phenocrysts of plagioclase, sanidine, and trace of biotite; 0–10 percent devitrified pumice; and 1–5 percent lithic clasts. Characterized by 5–15 percent flattened lithophysae. Unit includes crystal-poor lower lithophysal zone (Tptpll) of Buesch and others (1996). Thickness 41–91 m

tpln **Lower nonlithophysal zone**—Shown in cross sections only. Pale-red, grayish-red-purple, and pinkish-gray, densely welded, devitrified, rhyolitic ash-flow tuff. Contains 1–2 percent phenocrysts of plagioclase, sanidine, and trace of biotite; 1–15 percent devitrified pumice; and 1–5 percent lithic clasts. Unit

includes columnar subzone (Tptplnc) of Buesch and others (1996). Thickness 34–63 m

tpv **Vitric zone**—Shown in cross sections only. Grayish-black to light-gray, moderate-brown to grayish-brown to light-brown, and grayish-orange-pink, densely welded to nonwelded, vitric, rhyolitic ash-flow tuff. Contains 1–2 percent phenocrysts of plagioclase, sanidine, and trace of biotite; 0–15 percent pumice; and 2–10 percent lithic clasts, locally spherulitic. Unit includes following units of Buesch and others (1996): crystal-poor densely welded subzone (Tptpv3), crystal-poor moderately welded subzone (Tptpv2), and crystal-poor nonwelded subzone (Tptpv1). Thickness 25–67 m

Tac **Calico Hills Formation**—Shown in cross sections only. Pale-orange and grayish-yellow, nonwelded, vitric, rhyolitic ash-flow tuff, fallout tephra, and reworked bedded tuff. Contains 1–12 percent phenocrysts of sanidine, plagioclase, quartz, and biotite; locally as much as 40 percent pumice; and locally as much as 20 percent volcanic lithic clasts. Unit includes a basal volcaniclastic sandstone. As thick as 45 m

Crater Flat Group

Tcp **Prow Pass Tuff**—Shown in cross sections only. Light-gray to orange-pink to pale red and pale-yellowish-brown to moderate-brown, nonwelded to moderately welded, vitric to devitrified and altered, rhyolitic ash-flow tuff. Contains 7–11 percent phenocrysts of plagioclase, sanidine, quartz, biotite, and pyroxene pseudomorphs; 3–25 percent pumice; and 1–7 percent volcanic and red siltstone lithic clasts. Unit includes a basal bedded, reworked tuff. As thick as 135 m

ABSTRACT

New 1:6,000-scale geologic mapping in a 20-square-kilometer area near the south end of Yucca Mountain, Nevada, which is the proposed site of an underground repository for the storage of high-level radioactive wastes, substantially supplements the stratigraphic and structural data obtained from earlier, 1:24,000-scale mapping. Principal observations and interpretations resulting from the larger scale, more detailed nature of the recent investigation include: (1) the thickness of the Miocene Tiva Canyon Tuff decreases from north to south within the map area, and the lithophysal zones within the formation have a greater lateral variability than in areas farther north; and (2) fault relations are far more complex than shown on previous maps, with both major (block-bounding) and minor (intrablock) faults showing much lateral variation in (a) the number of splays and (b) the amount, distribution, and width of anastomosing breccia and fracture zones.

INTRODUCTION

Geologic mapping at a scale of 1:6,000 was conducted in a 20-km^2 area near the south end of Yucca Mountain, Nev. This area may be included in the proposed repository for high-level radioactive wastes (fig. 1). The map area includes most of Abandoned Wash, the southern part of Yucca Mountain, the northern parts of Iron Ridge and Forlorn Wash, and much of Dune Wash (fig. 2). The mapping supplements existing, less-detailed stratigraphic and structural data presented on the 1:24,000-scale map of Day, Dickerson, and others (1998). The present map is one of a series of bedrock geologic maps at the 1:6,000 scale that includes the central part of Yucca Mountain (Day, Potter, and others, 1998) and an area north of Yucca Wash (Dickerson and Drake, 1998). Previously mapped areas and the outlines of regional geologic map compilations are shown in figure 3. Map units on all of these maps, mostly pyroclastic-flow and fallout tephra deposits of the Miocene Timber Mountain and Paintbrush Groups, follow the formal nomenclature of Sawyer and others (1994) and the informal units of Buesch and others (1996).

The map and report were prepared in cooperation with the Yucca Mountain Site Characterization Office, U.S. Department of Energy, under Interagency Agreement DE-AI08-02RW12167.

PREVIOUS MAPPING

The first detailed geologic maps of the Yucca Mountain region resulted from systematic 1:24,000-scale geologic mapping of quadrangles in and near the Nevada Test Site, conducted by the U.S. Geological Survey in the late 1950's. The geologic map of the Topopah Spring SW quadrangle by Lipman and McKay (1965) covers the present map area at a scale of 1:24,000 (fig. 3). Several smaller scale subregional geologic

maps that include the area of the present map were subsequently compiled. All of these compilations were based on the earlier 1:24,000-scale geologic maps and include the 1:48,000-scale geologic map of the Jackass Flats area by Maldonado (1985), the 1:100,000-scale geologic map of the Nevada Test Site by Frizzell and Shulters (1990), and the digital geologic map of the Nevada Test Site area by Wahl and others (1997).

In the early stages of site characterization at Yucca Mountain more detailed geologic mapping efforts resulted in the 1:12,000-scale preliminary geologic map of Yucca Mountain by Scott and Bonk (1984) (fig. 3). This map provided considerably more structural and stratigraphic detail than the previous geologic maps of Yucca Mountain. In addition to displaying a larger number of faults with smaller amounts of offset than was shown on the Lipman and McKay (1965) map, this was the first map to portray zonal characteristics of the Paintbrush Group welded tuffs at Yucca Mountain. The Scott and Bonk (1984) map extends only into the very northern part of the map area. A similarly detailed map of the southern half of Yucca Mountain was produced by Scott (1992) (fig. 3). Simonds and others (1995) compiled a 1:24,000-scale fault map of Yucca Mountain, integrating new data on Quaternary to Holocene fault activity with bedrock faults mapped by Scott and Bonk (1984) and R.B. Scott (USGS, unpub. mapping,1992).

More recently, detailed bedrock geologic maps have been completed in support of site characterization for various parts of the Yucca Mountain area that use the most recent informal stratigraphic nomenclature of Buesch and others (1996). These include the bedrock geologic map of the central block of Yucca Mountain by Day, Potter, and others (1998) at a scale of 1:6,000, and the geologic map of the Paintbrush Canyon area by Dickerson and Drake (1998) at the same scale (fig. 3). The results from additional geologic mapping of Yucca Mountain are presented in the bedrock geologic map of the Yucca Mountain area by Day, Dickerson, and others (1998) at a scale of 1:24,000, and in the geologic map of the Yucca Mountain region by Potter and others (2002) at a scale of 1:50,000 (fig. 3).

METHODS

Geologic mapping

Observations were recorded on 1:6,000-scale orthophoto maps prepared specifically for Yucca Mountain site characterization studies. Digital orthophoto maps were loaded into a hand-held pocket computer that was linked to a global positioning system (GPS) receiver. Location data and any other data associated with specific geologic features were digitally recorded. The advertised autonomous accuracy of the GPS receiver used to make this map is 10 m in the horizontal direction. However, during numerous equipment tests, the GPS accuracy was commonly found to be equal to the resolution of the digital orthophotos, or about 3-m accuracy. Previous geologic mapping was useful for locating and defining the principal structures within the map area, and for identifying the main lithostratigraphic units encountered in the northern part of the map area. The present map is primarily a bedrock geologic map, with Quaternary surficial deposits broadly classed as alluvium and (or) colluvium.

Faults having a displacement of 2 m or more are portrayed on the map where recognized, although fault segments of lesser displacement are shown where needed to clarify contact relations between map units, or along terminal segments of a larger fault where displacement diminishes to imperceptible. Faults with much less than 2 m of offset are easily recognized where they offset bedded tuffs, but faults with greater than 2 m of offset may be unrecognized where they lie completely within a thick, homogeneous unit such as the middle nonlithophysal zone of the Tiva Canyon Tuff. Structures beneath the surficial deposits are inferred, based on extrapolation from outcrops and from local geophysical data.

Detailed mapping was conducted from November 2001 to May 2002. The mapping was largely confined to the area between Dune Wash and the western side of Yucca Mountain and Iron Ridge. The results of this detailed mapping are presented at a scale of 1:6,000. Our map also includes data from the previously published 1:24,000-scale bedrock geologic map of the Yucca Mountain area (Day, Dickerson, and others, 1998) reproduced here at a scale of 1:6,000 for the area east of Dune Wash, southeast of East Ridge, and in lower Solitario Canyon and WT-11 Wash. These geologic data are provided as context for the newer, more detailed mapping. A blue line separates the newer 1:6,000-scale mapping from the previous 1:24,000-scale mapping.

Geophysical data

Regional gravity and magnetic data were found to be of little use in delineating structures

beneath surficial deposits in the map area, but local, ground-based surveys provided more meaningful data on subsurface relations. The Dune Wash magnetic traverse of Ponce (1996) lies adjacent to the northern and eastern boundaries of the map area. The locations of magnetic anomalies along this traverse correlate well with faults exposed in bedrock because of the fault juxtaposition of the normally polarized Topopah Spring Tuff, the reversely polarized Tiva Canyon Tuff, and the normally polarized Rainier Mesa Tuff. These magnetic relations helped locate the Dune Wash fault where it was covered by surficial deposits (Ponce, 1996, pl. 2).

REGIONAL SETTING

Yucca Mountain is located about 140 km northwest of Las Vegas, Nev., and about 40 km east of Death Valley, Calif. (fig. 1). The area set aside by the U.S. Department of Energy for site characterization studies for the proposed underground storage of high-level radioactive waste lies partially within the Nevada Test Site, partially within Nellis Air Force Base Bombing and Gunnery Range, and partially on Bureau of Land Management land. The landscape consists of gently east dipping questas and ridges of volcanic rock surrounded by alluvial basins and dry arroyos.

Yucca Mountain lies directly south of the Miocene Timber Mountain–Claim Canyon caldera complex (fig. 1), within the southwest Nevada volcanic field. Volcanic rocks of the southwest Nevada volcanic field range in age from 15 to 9 Ma, and were erupted from several calderas and caldera complexes within the volcanic field (Sawyer and others, 1994). The volcanic field is dominated by rhyolites and latites, with subordinate amounts of andesite and basalt. Small-volume basaltic cinder cones and lava flows of late Tertiary and early Quaternary age also were erupted near Yucca Mountain in Crater Flat. The tuffs that compose Yucca Mountain largely originated from calderas in the Timber Mountain–Claim Canyon caldera complex that lies just north of Yucca Mountain (fig. 1).

Yucca Mountain also lies within the Walker Lane belt, a northwest-trending zone of deformation dominated by dextral shear strain and crustal extension (Stewart, 1988). Northwest-striking strike-slip faults associated with Walker Lane deformation include the Las Vegas Valley shear zone southeast of Yucca Mountain and the Stewart Valley/State Line fault south of Yucca Mountain (fig. 1). Death Valley lies southwest of Yucca Mountain and is a zone of Neogene crustal extension that is characterized by northwest-trending strike-slip faults, low-angle detachment faults, and high-angle normal faults. More modest amounts of crustal extension at Yucca Mountain are expressed by the Bare Mountain fault to the west, the "gravity fault" to the east, and the north-striking normal faults of Yucca Mountain between them (fig. 1). There are major detachment faults at Bare Mountain (Fluorspar Canyon and Bullfrog Hills detachments) and the Funeral Mountains (Boundary Canyon detachment) west of Yucca Mountain, and a minor detachment fault southeast of Yucca Mountain at the Point-of-Rocks (fig. 1).

STRATIGRAPHY

STRATIGRAPHIC NOMENCLATURE

The stratigraphic nomenclature used on this map is modified from that presented in Buesch and others (1996) for the informal units, and slightly modified from that used by Day, Potter, and others (1998). These modifications were made to provide a less cumbersome method of denoting mappable lithostratigraphic units for both the map and the cross sections. Typically the Tiva Canyon Tuff is referred to with the symbol "Tpc" and the Topopah Spring Tuff is referred to with "Tpt" (see for example, Christiansen and Lipman, 1965; Lipman and McKay, 1965; Maldonado, 1985; Potter and others, 2002). This basic nomenclature was greatly expanded upon by Buesch and others (1996) to better meet diverse needs for identification of informal members, zones, subzones, and intervals within the Tiva Canyon and Topopah Spring Tuffs for site characterization studies. Following Day, Potter, and others (1998), map units are designated as "c" for Tiva Canyon Tuff and "t" for Topopah Spring Tuff, as well as "r" and "p" for crystal-rich and crystal-poor members, respectively. Additional letters are used to delineate zones because they are useful for defining structures at a scale of 1:6,000. With a few exceptions, subzones are not mapped at this scale. One mappable subzone in the Tiva Canyon Tuff is the "columnar subzone of the lower nonlithophysal zone," which forms a prominent and easily identifiable bench near the base of the Tiva Canyon Tuff. Two other subzones were mapped locally where they formed useful map units, as discussed below.

TERTIARY STRATIGRAPHY

The Tertiary stratigraphic units of the Yucca Mountain area consist of Miocene rhyolite tuffs and lavas of the 13.25 Ma Crater Flat Group, the 13.0 Ma Wahmonie Formation, the 12.9 Ma Calico Hills Formation, the 12.7–12.8 Ma Paintbrush Group, the 12.5–11.45 Ma Timber Mountain Group (Sawyer and others, 1994), and minor amounts of younger basaltic lava flows (Crowe and others, 1995). All of these units are exposed at the surface and encountered in the subsurface in drill holes at and around Yucca Mountain. Drill holes in and around the map area indicate that the descending Calico Hills Formation and the Prow Pass, Bullfrog, and Tram Tuffs of the Crater Flat Group all exist at depth, but the Wahmonie Formation does not (Scott and Castellanos, 1984; R. Spengler and D. Buesch, written commun. to R. Craig, 1997). Paintbrush Group rocks are widely exposed in the map area and are described in greater detail below. Exposures of Timber Mountain Group rocks are extremely limited within the boundaries of the map area, but they do exist in a north-south-striking paleovalley along the Solitario Canyon fault and along Dune Wash on the hanging wall of the Bow Ridge fault.

At Yucca Mountain, the Paintbrush Group is typically made up of four principal extra-caldera ash-flow tuffs and their associated small volume fallout deposits and local surge deposits, as well as several other smaller volume pyroclastic flow deposits. From oldest to youngest, the principal ash-flow tuffs are the Topopah Spring Tuff, the Pah Canyon Tuff, the Yucca Mountain Tuff, and the Tiva Canyon Tuff. Pumice and ash fallout deposits are usually located at the base of each major ash-flow tuff, and locally may be preserved at the top as well. Surge deposits are located only at the base of the ash-flow deposits, and usually are located within a few kilometers of the eruptive source. Each of the four major ash-flow deposits is densely welded tuff over some part of its areal distribution, and locally exhibits lithophysal zones within the densely welded interior of the tuff. The largest volume ash-flow tuffs within the Paintbrush Group are the Tiva Canyon Tuff and the Topopah Spring Tuff, which are moderately to densely welded throughout most of their areas of distribution. In addition to these major out-flow sheets, some of these welded tuffs also have intracaldera facies that are exposed as thick deposits of densely welded tuff north and northwest of Yucca Mountain in the Claim Canyon caldera segment of the Timber Mountain caldera complex (Byers and others, 1976; Potter and others, 2002). The Paintbrush Group also contains many smaller volume deposits of ash-flow tuff, fallout tuff, and local lava flows and domes proximal to the caldera complex in the northern part of Yucca Mountain (Dickerson and Drake, 1998).

The Topopah Spring and Tiva Canyon Tuffs dominate the exposed bedrock geology in the map area, which is located about 10 km south of the Claim Canyon caldera segment of the Timber Mountain caldera complex. Thin deposits of bedded tuff between these two thick welded tuffs, and minor deposits of nonwelded to moderately welded Rainier Mesa Tuff of the Timber Mountain Group are also present. At this distance south of the source caldera both the Pah Canyon Tuff and the Yucca Mountain Tuff have pinched out as mappable stratigraphic units (Day, Potter, and others, 1998), except for thin (few centimeters) nonwelded distal edges of the ash-flow deposits and possible associated fallout tephra within the bedded tuff. There are no surge deposits associated with any of the ash-flow tuffs at this distance from the caldera.

In the map area the Topopah Spring and Tiva Canyon Tuffs are thick welded tuffs consisting of a crystal-rich quartz latite upper member and a crystal-poor rhyolite lower member. The members of the Topopah Spring and Tiva Canyon Tuffs can be subdivided into mappable zones based on such criteria as pumice content, crystal content, welding and devitrification features, and the presence or absence of lithophysae (Buesch and others, 1996; Day, Potter, and others, 1998). Borehole G-3 (table 1), located on Yucca Mountain (fig. 2), revealed that the basal vitric zone (unit **tpv**), the lower nonlithophysal zone (unit **tpln**), and the lower lithophysal zone (unit **tpll**) of the crystal-poor member of the Topopah Spring Tuff exist at depth within the map area (R. Spengler and D. Buesch, written commun. to R. Craig, 1997; Scott and Castellanos, 1984). Bedrock exposures of the Topopah Spring Tuff consist of the middle nonlithophysal zone (unit **tpmn**) and the upper lithophysal zone (unit **tpul**) of the crystal-poor member, and the nonlithophysal zone (unit **trn**) and the vitric zone and the densely welded zone (unit **trv**) of the crystal-rich member. The crystal-rich lithophysal zone (unit **trl**) is locally present on a limited basis within the Dune Wash graben.

Throughout the map area the crystal-poor member of the Tiva Canyon Tuff consists of the basal vitric zone (unit **cpv**), the lower nonlithophysal zone (unit **cpln**), the lower

lithophysal zone (unit **cpll**), and the middle nonlithophysal zone (unit **cpmn**); and the crystal-rich member consists predominantly of the transition zone (unit **cr1**) and the mixed-pumice zone (unit **cr2**). Locally the columnar-jointed subzone of the lower nonlithophysal zone (unit **cplnc**), the middle lithophysal zone (unit **cpml**), the upper nonlithophysal zone (unit **cpun**), the upper lithophysal zone (unit **cpul**), the pumice-poor zone (unit **cr3**), and the vitric and subvitric transition zone (unit **cr4**) are present on a rather limited basis within the map area. All of the above zones in the Tiva Canyon Tuff are common to the geologic map of the central block of Yucca Mountain (Day, Potter, and others, 1998) except for the middle lithophysal zone of the crystal-poor member (unit **cpml**); these stratigraphic units are discussed in greater detail below.

The Topopah Spring and Tiva Canyon Tuffs both exhibit lateral facies variations that effect changes in zonal features throughout Yucca Mountain. In the central block of Yucca Mountain, for example, the Tiva Canyon Tuff exhibits an upper lithophysal zone (unit **cpul**) that extends upward across the contact between the crystal-rich member and the crystal-poor member (fig. 4), and the lower half of the crystal-rich member is predominantly lithophysae bearing (Potter and others, 1999). In contrast, the upper lithophysal zone in the southern part of the map area is thin and sparsely distributed, pinching out laterally. However, the lower half of the crystal-rich member commonly contains abundant lithophysae. In the central block of Yucca Mountain, the crystal-poor member of the Tiva Canyon Tuff also exhibits a middle nonlithophysal zone (unit **cpmn**) that locally develops an upper nonlithophysal subzone (unit **cpun**), a thin middle lithophysal subzone (unit **cpml**), and a lower nonlithophysal subzone (unit **cpln**), whereas farther south, these subzones develop into thick, mappable zones—the upper nonlithophysal zone (unit **cpun**), the middle lithophysal zone (unit **cpml**), and the middle nonlithophysal zone (unit **cpmn**) (fig. 4). The crystal-poor member's lower lithophysal zone (unit **cpll**) changes thickness and lithophysae concentration, and locally is a zone dominated by vapor-phase partings with sparse lithophysae, or is a zone with a lower lithophysae-rich part and an upper lithophysae poor part. The lateral changes in the lower lithophysal zone commonly accompany changes in the middle nonlithophysal zone, including thickness changes and local development of a separate lithophysal subzone (fig. 4).

Lateral changes in thickness and zonal characteristics of the Tiva Canyon Tuff take place over distances of less than a kilometer. Overall, the Tiva Canyon Tuff and the subjacent bedded tuff become thinner from the northwest to the southeast, although changes in thickness of the bedded tuff are less pronounced than the thickness changes in the Tiva Canyon Tuff. The crystal-rich member's pumice-poor zone (unit **cr3**) and vitric and subvitric transition zone (unit **cr4**) exist at the top of the Tiva Canyon Tuff in the southeast corner of the map, east of East Ridge, and are locally preserved in down-faulted blocks in fault zones throughout the map area. From north to south, the crystal-rich member's transition zone (unit **cr1**) and mixed pumice zone (unit **cr2**) become thinner and the size of the pumice clasts within the mixed pumice zone diminishes. Lithophysae are distributed in both units **cr1** and **cr2**, and the base of this lithophysal zone varies from just below the basal unit **cr2** contact to 8 m below the basal unit **cr1** contact. The crystal-poor member's upper lithophysal zone (unit **cpul**) is recognized and mapped where this lithophysal zone extends into the crystal-poor member of the Tiva Canyon Tuff in Dune Wash, northern Abandoned Wash, and Forlorn Wash.

Buesch and others (1996) defined the lithophysae-bearing subzone of the crystal-poor member's middle nonlithophysal zone (Tpcpmn2). This subzone forms a distinct map unit (the crystal-poor member's middle lithophysal zone—unit **cpml**) in the southern part of the map area (fig. 4). In most places, the middle nonlithophysal zone consists of a blocky upper part characterized by a conchoidal fracture and a flaky lower part characterized by a hackly fracture. However, in the southernmost part of the map area, the middle nonlithophysal zone consists only of the blocky part, with a small blocky ledge at the base of the zone. The lithophysae-bearing subzone of the crystal-poor member's middle nonlithophysal zone (unit **cpmn**) is locally developed within this blocky ledge, and thickens laterally to become the middle lithophysal zone (unit **cpml**) (fig. 4). The middle lithophysal zone is recognized on Double Notch Ridge, on Silica Ridge, and on Canis Ridge at this stratigraphic horizon, where irregularly shaped lithophysae 4–10 cm in diameter are relatively abundant.

The crystal-poor member's lower lithophysal zone (unit **cpll**) is thickest (27 m) in the northwestern part of the map area beneath Yucca Crest, but generally becomes thinner towards the south beneath Double Notch Ridge (6 m). In the northern part of the map area, the

lower lithophysal zone is dominated by small oblate lithophysae 2–4 cm in diameter, but contains numerous vapor-phase partings at the upper and lower contacts. In the central part, lithophysal cavities are still concentrated toward the center of the zone but vapor-phase partings compose a larger part of the upper and lower parts of the lithophysal zone. As the lower lithophysal zone (unit **cpll**) thins to the south, vapor-phase partings increase as the total number of lithophysae decrease, and lithophysae are concentrated in the lower part of the lower lithophysal zone. Locally, such as on the southern part of Abandoned Ridge, sparse lithophysae and vapor-phase partings extend upward to the base of the lithophysae-bearing subzone of the middle nonlithophysal zone, making the lower lithophysal zone appear unusually thick. In the southernmost part of the map area, on Double Notch Ridge, the lower lithophysal zone is much thinner and dominated by lithophysal cavities, with vapor-phase partings extending upwards through much of the middle nonlithophysal zone (fig. 4).

The crystal-poor member's lower nonlithophysal zone (unit **cpln**) is thickest in Dune Wash (24 m) and is characterized in most places by hackly fractured rock that erodes into small irregular chips. In the Forlorn Wash area, however, this unit exhibits lateral changes to a blocky morphology that exhibits a conchoidal fracture identical to that of the middle nonlithophysal zone, and these lateral changes take place over distances of a few meters. In the southeast quarter of the map, on Silica Ridge and Canis Ridge, the lower part of the lower nonlithophysal zone forms a small cliff that is not related to the columnar-jointed subzone. The columnar subzone of the lower nonlithophysal zone (unit **cplnc**) exists only intermittently in northern Dune Wash, Abandoned Wash, Forlorn Wash, and on Double Notch Ridge, where it commonly forms a bench or a small cliff. The crystal-poor member's basal vitric zone (unit **cpv**) is composed of nonwelded to partly welded vitric tuff that is a distinctive yellowish-orange color throughout most of the map area. However, on the northeast side of Silica Ridge, this zone is black to very dark gray and includes a moderately to densely welded basal vitrophyre.

Subsurface lithostratigraphic data from drill holes (Scott and Castellanos, 1984; Kume and Hammermeister, 1991; R. Spengler and D. Buesch, written commun. to R. Craig, 1997) are used here to describe the Calico Hills Formation and the underlying Prow Pass Tuff, inasmuch as these formations underlie the Topopah Spring Tuff as shown on the accompanying geologic cross sections. The Calico Hills Formation is a pumice- and lithic-rich, nonwelded, vitric, ash-flow tuff that is underlain by bedded tuff (Scott and Castellanos, 1984). Bedrock exposures on the north side of Busted Butte show that this ash-flow tuff is composed of five distinct pyroclastic flow deposits, and the bedded tuff is a complex package of primary pumice and ash fallout deposits and reworked ash-flow deposits overlying a distinctive volcaniclastic sandstone (Moyer and Geslin, 1995). The Prow Pass Tuff of the Crater Flat Group is a lithic-rich, vitric to devitrified, nonwelded to partly welded ash-flow tuff that contains distinctive lithic clasts composed of red mudstone. The Prow Pass Tuff is underlain by a bedded tuff sequence composed of pyroclastic fallout and flow deposits, and interbedded volcaniclastic sedimentary rocks (Scott and Castellanos, 1984).

QUATERNARY STRATIGRAPHY

Numerous thin alluvial, colluvial, slope-failure, rock-fall, and talus deposits of Quaternary age exist throughout the map area. Alluvium and colluvium forming unconsolidated deposits of silt, sand, gravel, and cobbles in washes, on floodplains, and on low sloping hills are mapped together as unit **Qac**. These deposits extend partway up the gentle slopes on the sides of washes where they become thin and mixed with in-situ debris weathered from the underlying bedrock. The contact between unit **Qac** and bedrock is identified in the field where allochthonous debris predominates over bedrock or autochthonous debris derived from in-situ weathering of bedrock. Poorly developed desert pavement is found locally on surficial deposits within the map area.

Slope-failure and debris-flow deposits exist on steep slopes and in narrow, steep gullies, and talus cones are localized at the base of cliffs. In situ weathered talus deposits are especially characteristic of the middle nonlithophysal zone of the Tiva Canyon Tuff (unit **cpmn**). Slope-failure and debris-flow deposits are characterized by clasts of various sizes, and by lobate geomorphic forms in their lower parts. Talus deposits are cone shaped at the base of small cliffs or steep slopes, but compose broad, irregularly shaped areas of loose rock at the mid-slope level. These latter deposits contain large tabular blocks that are commonly stained dark brown to black by desert varnish, and form prominent black "rock stripes" on the sides of narrow canyons and washes, and on steep slopes. North-facing and west-facing slopes

appear to contain more of these distinctive "rock-stripe" talus deposits than do east-facing and south-facing slopes. All of these deposits are lumped together as colluvial map unit Qc.

STRUCTURE

The structure of Yucca Mountain is dominated by north-striking normal faults that resulted from the tectonic development of the Crater Flat basin concomitant with eruption of some of the voluminous pyroclastic material from the Timber Mountain caldera complex (Fridrich and others, 1999). North-striking normal faults generally with more than 100 m of vertical offset have divided Yucca Mountain into distinct east-dipping fault blocks, and these faults are categorized as block-bounding faults. Some of the block-bounding faults are linked by northwest-striking relay structures that exhibit down-to-the-southwest normal offset, and acted to transfer displacement from one block-bounding fault system to another (Day, Dickerson, and others, 1998). Within each fault block local strain was accommodated by smaller intrablock faults that exhibit a few meters to a few tens of meters of offset. Both block-bounding faults and intrablock faults locally display zones of deformation that widen upward to the surface as systems of upward-splaying faults and anastomozing breccia zones (Spengler and others, 1993; Day, Dickerson, and others, 1998; Day, Potter, and others, 1998). In northern Yucca Mountain modest amounts of right-lateral displacement occurred on northwest-striking strike-slip faults, but such faults are not present in the central and southern parts of Yucca Mountain (Day, Dickerson, and others, 1998).

BLOCK-BOUNDING FAULTS

Block-bounding faults are the largest faults present in the map area and commonly show more than 200 m of vertical offset. These faults generally strike within 15° of true north, and dip from 45° to 75° west. Block-bounding faults display great lateral variability by commonly splaying into numerous fault strands, exhibiting hanging-wall grabens, tectonic fault slivers, and areas of pervasive hanging-wall brecciation (Scott and Bonk, 1984; Scott, 1992; Dickerson and Spengler, 1994; Day, Dickerson, and others, 1998; Dickerson and Drake, 1998). Locally, block-bounding faults are kinematically linked by northwest-striking relay structures composed of several closely spaced down-to-the-southwest normal faults. Slickensides preserved on fault scarps indicate that movement on block-bounding faults was oblique slip down to the southwest (Scott and Bonk, 1984; Scott, 1992; Day, Potter, and others, 1998; Dickerson and Drake, 1998).

Regional structural data show that the number of block-bounding faults, the aggregate amount of offset across these faults, and the width of each fault zone all increase systematically from north to south at Yucca Mountain, and that the dip of block-bounding faults systematically decreases from north to south (Potter and others, 2002; Scott, 1992). One effect of this southward increase in faulting at Yucca Mountain is to increase the total volume of rock that has been mechanically disrupted. Another potential result is to increase the degree of anisotropy in fracture-dominated subsurface flow from north to south at Yucca Mountain as fault zones increasingly channelize fluids.

The map area is bounded on the west by the block-bounding Solitario Canyon and Iron Ridge faults. The Dune Wash fault is the block-bounding fault on the east side of the map area, and forms one side of the Dune Wash graben. The East Ridge fault forms the west side of the Dune Wash graben in the eastern part of the map area. The Forlorn Wash fault is a block-bounding fault southwest of the Dune Wash graben and forms the strike valley of Forlorn Wash in the southeastern part of the map area (fig. 1).

INTRABLOCK FAULTS

Within each fault block, smaller north-striking and northwest-striking normal faults display a few meters to a few tens of meters of dip-slip movement. These faults have steeper dips, commonly 75°–90°, and exhibit fewer associated fault splays than do the block-bounding faults. Intrablock faults range in length from 100 m to several kilometers. Locally, they contain upward-widening zones of fault splays and discontinuous breccia zones (Potter and others, 1999). Some intrablock faults bound small grabens that preserve strata of higher stratigraphic units that were removed from adjoining blocks by erosion. Intrablock faults manifest lateral variability along strike in the amount of vertical offset, degree of brecciation, and number of related fault splays (Spengler and others, 1993; Day, Potter and others, 1998; Day, Dickerson, and others, 1998; Potter and others, 1999).

Within the map area the principal intrablock faults are the Abandoned Wash fault

in the center of the map area, several faults parallel to and east of the Forlorn Wash fault, and numerous smaller normal faults within the Dune Wash graben. A host of northwest-striking and northeast-striking smaller intrablock faults splay out of the Abandoned Wash fault, and several northwest- and northeast-striking intrablock faults splay out of the Forlorn Wash fault. Numerous north-striking and northeast-striking intrablock faults splay into the footwall of the Iron Ridge fault as well.

FAULT-ZONE ARCHITECTURE

A typical fault has an adjacent damage zone of fractured or brecciated rock that resulted from fault growth, and a fault core composed of clay gouge or breccia of finely comminuted material that accommodated the majority of fault displacement (Chester and Logan, 1987; Forster and Evans, 1991; Caine and others, 1996; Caine and Forster, 1999). Faults can contain a core zone with one or more polished fault surfaces, and locally contain no core zone at all (fig. 5). Damage zones, and core zones that lack gouge, produce significant volumes of fractured and brecciated rock that potentially affect underground engineering projects and act as conduits for subsurface fluid flow (Caine and others, 1996). Locally, core zones can be dominated by clay fault-gouge that acts as a barrier to cross-fault flow (Caine and others, 1996). Alteration and mineral precipitation within the fault zone can also affect rock properties within a fault zone and alter the hydrogeologic characteristics of fault zones by occluding pore space and filling connecting fractures. Field studies of fault zones indicate that most of the fault zone characteristics discussed above exist locally at Yucca Mountain (Dickerson and others, 1999; Dickerson, 2001).

Typically, both intrablock faults and block-bounding faults at Yucca Mountain contain damage zones with fractured and locally brecciated rock. The damage zones associated with block-bounding faults are much more extensive and wider than those associated with intrablock faults, some as much as 150 m wide. Data concerning the width of probable damage zones of block-bounding faults within the map area, however, are scarce, because of burial by surficial deposits, but such zones may be extensive. The Dune Wash graben and the Solitario Canyon fault contain local fault zones composed of numerous tectonic slivers, small grabens, and extensive breccia zones as much as 100 m wide. Typical damage zones associated with intrablock faults are a meter or two wide. Some intrablock fault splays associated with the Abandoned Wash fault have 30 m of vertical separation and contain breccia zones 1 m wide. The core zones of intrablock faults usually lack clay gouge, and instead are narrow breccia zones a few centimeters thick composed of more finely comminuted material than the breccia found within the surrounding damage zone.

There is much lateral and vertical variability between faults at Yucca Mountain, and some of this variability appears systematic. For example, block-bounding faults commonly have much wider damage zones than intrablock faults, and block-bounding faults with the greatest amount of offset contain the most pervasive damage zones. The orientation of fault segments also affects the degree and extent of damage zone development. Slickensides on block-bounding fault scarps throughout Yucca Mountain indicate left-oblique slip (Day, Dickerson, and others, 1998; Dickerson, 2001). Fault segments with a northwest strike create releasing bends with local regimes of transtension, and fault segments with a northeast strike create restraining bends with local regimes of transpression. Studies show that transtension results in dilational breccias that are more open and contain less fine-grained matrix material, whereas transpression results in crush breccias that are compressed and contain a higher percent of fine-grained matrix (Christie-Bick and Biddle, 1985; Sibson, 1986; and Sylvester and Smith, 1976).

Petrographic data show great variability for fault-zone breccias at Yucca Mountain. Breccias from block-bounding faults contain much smaller clast sizes and greater proportions of sand- and silt-size matrix material than breccias from intrablock faults. Samples of breccia collected from surface exposures all contain calcite cement, and some of them also contain silica cement. Breccia sampled from the underground workings of the Exploratory Studies Facility exhibit far less cement, and the majority of that cement is silica and clay (Dickerson, 2001). Clay gouge is observed in the core zone of the Solitario Canyon fault, and clay exists as cement and as matrix in damage zone breccias. Breccias from block-bounding faults, and to a lesser extent from intrablock faults, exhibit several cycles of rock fracturing and cementation, exhibited by early generation fractures that are partly to completely occluded by silica cement and by a later set of fractures that crosscut clasts, matrix, and older fractures, and that remain free of cement.

Several faults in the southern part of the Dune Wash graben exhibit pervasive silicification. Additionally, secondary silica is found on the surface along many of the faults of Silica Ridge adjacent to the Dune Wash graben. Here, the silica typically is white to colorless and botryoidal. The amount of secondary silica observed along the faults on Silica Ridge and in the southern part of the Dune Wash graben is much greater than that observed for both intrablock faults and block-bounding faults elsewhere in the map area.

DESCRIPTION OF INDIVIDUAL STRUCTURES

Solitario Canyon fault

The Solitario Canyon fault is a block-bounding fault that lies near the west side of the map area (fig. 2). It has a total length of about 22 km, extending from Chocolate Mountain north of Yucca Mountain to the Windy Wash fault in southern Crater Flat (fig. 1). Slickensides on fault scarps indicate left-oblique slip to the southwest (Scott and Bonk, 1984; Day, Potter, and others, 1998). Vertical separation is about 210 m down to the west at the north end of the map area, near Plug Hill (fig. 2) (see Day, Dickerson, and others, 1998). The Solitario Canyon fault strikes south to a point west of borehole UZ-13 (table 1) on Yucca Mountain, at which point the fault changes strike to the southwest, creating a restraining bend. It is at this restraining bend that the Iron Ridge fault splays from the Solitario Canyon fault in a series of northwest-striking relay faults (fig. 2). South of this point, total offset on the Solitario Canyon fault system continues to increase, but its main strand loses approximately 120 m of displacement to the Iron Ridge fault, another approximately 75 m of displacement to the northernmost unnamed splay, and another 30–60 m of displacement to each of several other unnamed faults that splay off into the footwall to the south-southeast. In surface exposures, the Solitario Canyon fault zone is about 500 m wide and includes more than nine separate fault splays and breccia zones in lower Solitario Canyon, just north of the map area (Day, Potter, and others, 1998). The Solitario Canyon fault zone remains wide, complex, and laterally variable to the south. However, because surficial deposits obscure the fault zone, the actual width of the fault zone south of the restraining bend is unknown. Drill-hole data from borehole WT-10 (R. Spengler and D. Buesch, written commun. to R. Craig, 1997), geophysical data (McCafferty and Grauch, 1997), and surface map data (Day, Dickerson, and others, 1998) indicate an estimated width of the fault zone within the map area that varies laterally from approximately 270 to 830 m. The complexity of this fault zone in bedrock exposures indicates that such complexly deformed rock likely exists in those areas covered by colluvium and alluvium.

Iron Ridge fault

The Iron Ridge fault is a block-bounding fault located in the southwestern part of the map area. This fault splays off the Solitario Canyon fault at a relay structure west of UZ-13 (table 1) and can be traced for a distance of 8.5 km adjacent to the west side of Iron Ridge. The fault has 120 m of cumulative vertical displacement at the point where it splays off the Solitario Canyon fault, and this displacement increases southward to about 185 m. One kilometer to the southeast of the splay point, nine different fault splays are within the Iron Ridge fault zone. Whereas most of these fault splays are less than a kilometer long, the Iron Ridge fault contains two near-parallel strands that traverse the full length of the fault zone and are between 300 and 400 m apart. Near the south edge of the map, the westernmost fault strand lies in the bottom of WT-11 Wash and has approximately 30 m of down-to-the-west offset, whereas the easternmost strand lies about 30 m higher up the east slope of WT-11 Wash and has about 155 m of down-to-the-west offset.

Dune Wash fault

The Dune Wash fault is a block-bounding fault that lies on the east edge of the map area. This fault extends from the north side of Broken Limb Ridge in the central block area southward into Dune Wash (see Day, Potter, and others, 1998, for details of the northern part of this fault). In upper Dune Wash just north of the map area, the fault zone contains at least three west-stepping fault strands, three separate fault zone grabens, and breccia zones in both hanging wall and footwall. There the entire fault zone is more than 30 m wide (Day, Potter, and others, 1998), with cumulative vertical displacement of about 50 m. Farther to the south in Dune Wash the fault is completely obscured by Quaternary valley-fill deposits. Subsurface lithostratigraphic data indicate approximately 210 m of down-to-the-west offset adjacent to borehole WT-1, which diminishes to

about 145 m southward adjacent to borehole WT#17 (based on surface geologic contacts and attitudes, and on borehole intercepts and lithostratigraphic thicknesses from R. Spengler and D. Buesch, written commun. to R. Craig, 1997). Aggregate offset of faults beneath Dune Wash is inferred to decrease to the south because of the net decrease in offset from borehole WT-1 to borehole WT#17, and on changes in the structural level of the rocks on either side of Dune Wash. For example, crystal-rich Tiva Canyon Tuff on the west side of Dune Wash is juxtaposed against crystal-rich Topopah Spring Tuff on the east side of the fault adjacent to borehole WT-1, but farther south the crystal-rich Tiva Canyon Tuff is adjacent to crystal-poor Tiva Canyon Tuff. South of borehole WT#17, crystal-poor Tiva Canyon Tuff crops out on the west side of Dune Wash and welded Rainier Mesa Tuff crops out on the east side, yielding an apparent eastside-down relation. It is not known how much faulting occurred on the Dune Wash fault prior to emplacement of the Rainier Mesa Tuff, but enough post-Rainier Mesa Tuff deformation occurred to tilt this tuff 16° to the east on the east side of the wash, compared to only a 5° eastward tilt for the Rainier Mesa Tuff on the west side of the wash. Furthermore, at the southeasternmost end of Dune Wash the contact between the Rainier Mesa and Tiva Canyon Tuffs is buried beneath Dune Wash on the northeast side of the wash but is exposed up the slope on the southwest side of the wash (Day, Dickerson, and others, 1998). We interpret these relations to infer a net southward decrease in the offset along the Dune Wash fault system.

Dune Wash graben

The complex Dune Wash graben is formed by the Dune Wash fault on the east side and the East Ridge fault system on the west side. There are numerous down-to-the-east and down-to-the-west normal faults within the graben. The East Ridge fault is a small intrablock fault with a few meters of down-to-the-east displacement near the mouth of Abandoned Wash. Toward the south this fault is an increasingly complex structure as much as 100 m wide, with numerous anastomozing fault strands, tectonic slivers, and small hanging-wall grabens within the fault zone and numerous fault splays projecting into the country rock adjacent to it. There is a maximum of 146 m of cumulative down-to-the-east vertical separation on the East Ridge fault. Within the Dune Wash graben, normal faults create a series of smaller fault blocks within which strata tilt predominantly to the east, as well as several discontinuous smaller grabens and horst blocks. The Dune Wash graben probably terminates against the Paintbrush Canyon fault to the southeast, but Quaternary valley-fill deposits obscure this part of the structure.

Forlorn Wash fault and associated faults

The Forlorn Wash fault forms a complex system of mostly down-to-the-west faults located on the east side of Forlorn Wash in the southern part of the map area (fig. 2). Between this and the down-to-the-east East Ridge fault system is a wedge-shaped horst that includes Silica Ridge, Canis Ridge, and East Ridge. At the north end of this horst, two faults of the Forlorn Wash fault system merge into a complex part of the Dune Wash graben that is characterized by numerous closely spaced down-to-the-east and down-to-the-west faults. The Forlorn Wash fault system comprises two main down-to-the-west normal faults with numerous major and minor fault splays, one of which is located in the bottom of the wash and the other located on the west-facing slope of Silica Ridge. Just to the east of the main strand, located on the west-facing slope in Forlorn Wash, there is another complex fault that is predominantly down to the east. This fault originates on the east side of Silica Ridge and strikes to the southwest through the top of the ridge. On the west side of Silica Ridge this down-to-the-east fault strikes to the south, where it approximately parallels the two main faults of the Forlorn Wash fault system. Another pair of down-to-the-west faults lies a few hundred meters to the east of the down-to-the-east fault, forming a graben at the top of Silica Ridge. The major north-striking normal faults of the Forlorn Wash fault system are connected by numerous northeast-striking faults that bound several smaller grabens and fault blocks, yielding an area 0.5–1.0 km wide and 2 km long of faulted, brecciated, and fractured rock between Forlorn Wash and WT-12 Wash. The Forlorn Wash fault zone has a cumulative down-to-the-west displacement of about 80 m at the head of Forlorn Wash. At the southern edge of the map the various down-to-the-east and down-to-the-west faults have converged into a few faults within a zone 60 m wide in the bottom of Forlorn Wash that have a maximum cumulative down-to-the-west offset of about 110 m.

Abandoned Wash fault

The north-south-striking Abandoned Wash fault extends from Broken Limb Ridge (fig. 2) in the central part of Yucca Mountain (Day, Potter, and others, 1998) southward through upper Abandoned Wash and South Wash, eventually joining with the Iron Ridge fault just south of Double Notch Ridge (Day, Dickerson, and others, 1998) for a total length of 6 km. The Abandoned Wash fault is closely related to the Ghost Dance fault to the north, and likely represents the southern extension of this fault system (Day, Dickerson, and others, 1998). North of the map area, on Broken Limb Ridge, these two faults lie within 70 m of each other, have the same sense of offset, and likely are joined at depth (Day, Potter, and others 1998). In bedrock exposures in Abandoned Wash just north of the area of this map, the Abandoned Wash fault exhibits 24 m of down-to-the-west offset across a fault scarp that dips 81° west. The fault is characterized by a 2.4-m-wide breccia zone that becomes more finely comminuted in the center of the zone. On the north side of Abandoned Wash the fault variously exhibits one to two fault splays. For most of the length of Abandoned Wash the fault is obscured by surficial deposits, but in the saddle between South Wash and Abandoned Wash it has three parallel north-striking fault splays in a fault zone as wide as 38 m. The Abandoned Wash fault has 21 m of cumulative down-to-the-west displacement in the saddle between Abandoned Wash and South Wash. Numerous small northwest-striking faults ranging in vertical separation from 1 to 4 m splay off the main fault into the footwall on the east side of South Wash. Offset decreases to the south, but the fault still exhibits cumulative down-to-the-west displacement of about 8 m across three fault splays on Double Notch Ridge at the south edge of the map area.

REFERENCES CITED

Buesch, D.C., Spengler, R.W., Moyer, T.C., and Geslin, J.K., 1996, Proposed stratigraphic nomenclature and macroscopic identification of lithostratigraphic units of the Paintbrush Group exposed at Yucca Mountain, Nevada: U.S. Geological Survey Open-File Report 94–469, 45 p.

Byers, F.M., Jr., Carr, W.J., Orkild, P.P., Quinlivan, W.D., and Sargent, K.A., 1976, Volcanic suites and related cauldrons of the Timber Mountain–Oasis Valley caldera complex, southern Nevada: U.S. Geological Survey Professional Paper 919, 70 p.

Caine, J.S., Evans, J.P., and Forster, C.B., 1996, Fault zone architecture and permeability structure: Geology, v. 24, no. 11, p. 1025–1028.

Caine, J.S., and Forster, C.B., 1999, Fault zone architecture and fluid flow—Insights from field data and numerical modeling *in* Haneberg, W.C., Mozley, P.S., Moore, J.C., and Goodwin, L.B., eds., Faults and subsurface fluid flow in the shallow crust: Geophysical Monograph 113, p. 101–127.

Chester, F.M., and Logan, J.M., 1987, Composite planar fabric of gouge from the Punchbowl fault, California: Journal of Structural Geology, v. 9, no. 5/6, p. 621–634.

Christiansen, R.L., and Lipman, P.W., 1965, Geologic map of the Topopah Spring NW quadrangle, Nye County, Nevada: U.S. Geological Survey Geologic Quadrangle Map GQ–444, scale 1:24,000.

Christie-Bick, Nicholas, and Biddle, K. T., 1985, Deformation and basin formation along strike-slip faults: Society of Economic Paleontologists and Mineralogists Special Publication 37, p. 1034.

Crowe, B., Perry, F., Geisman, J., McFadden, L., Wells, S., Murrell, M., Poths, J., Valentine, G.A., Bowker, L., and Finnegan, K., 1995, Status of volcanism studies for the Yucca Mountain site characterization project: Los Alamos National Laboratory Report LA-12908-MS, 379 p.

Day, W.C., Dickerson, R.P., Potter, C.J., Sweetkind, D.S., San Juan, C.A., Drake II, R.M., and Fridrich, C.J., 1998, Bedrock geologic map of the Yucca Mountain area, Nye County, Nevada: U.S. Geological Survey Geologic Investigations Series Map I–2627, scale 1:24,000, 21-p. pamphlet.

Day, W.C., Potter, C.J., Sweetkind, D.S., Dickerson, R.P., and San Juan, C.A., 1998, Bedrock geologic map of the central block area, Yucca Mountain, Nye County, Nevada: U.S. Geological Survey Miscellaneous Investigations Series Map I–2601, scale 1:6,000, 15-p. pamphlet.

Dickerson, R.P., 2001, Hydrogeologic characteristics of faults at Yucca Mountain, Nevada, *in* High-level radioactive waste management—Proceedings of the Ninth International Conference, Las Vegas, Nev., April 29–

May 3, 2001: LaGrange, Ill., American Nuclear Society, one CD-ROM.
Dickerson, R.P., and Drake II, R.M., 1998, Geologic map of the Paintbrush Canyon area, Yucca Mountain, Nevada: U.S. Geological Survey Open-File Report 97–783, scale 1:6,000, 25-p. pamphlet.
Dickerson, R.P., and Spengler, R.W., 1994, Structural character of the northern segment of the Paintbrush Canyon fault, Yucca Mountain, Nevada, *in* High- level radioactive waste management—Proceedings of the Fifth International Conference, Las Vegas, Nev., May 22–26, 1994: LaGrange, Ill., American Nuclear Society, p. 2367–2372.
Forster, C.B., and Evans, J.P., 1991, Hydrogeology of thrust faults and crystalline thrust sheets—Results of combined field and modeling studies: Geophysical Research Letters, v. 18, no. 5, p. 979–982.
Fridrich, C.J., Jr., Whitney, J.W., and Hudson, M.R., 1999, Space-time patterns of late Cenozoic extension, vertical axis rotation, and volcanism in the Crater Flat basin, southwest Nevada, *in* Wright, L.A., and Troxel, B.W., eds., Cenozoic basin in the Death Valley region: Geological Society of America Special Paper 333, p. 197–212.
Frizzell, V.A., Jr., and Shulters, J., 1990, Geologic map of the Nevada Test Site, southern Nevada: U.S. Geological Survey Miscellaneous Investigations Service Map I–2046, scale 1:100,000.
Hamilton, W.B., 1988, Detachment faulting in the Death Valley region, California and Nevada, *in* Carr, M.D., and Yount, J.C., eds., Geologic and hydrologic investigations of a potential nuclear waste disposal site at Yucca Mountain, southern Nevada: U.S. Geological Survey Bulletin 1790, p. 221.
Kume, Jack, and Hammermeister, D.P., 1991, Geohydrologic data from drill-bit cuttings and rotary cores from test hole USW UZ-13, Yucca Mountain, Nevada: U.S. Geological Survey Open-File Report 90–362, 30 p.
Lipman, P.W., and McKay, E.J., 1965, Geologic map of the Topopah Spring SW quadrangle, Nye County, Nevada: U.S. Geological Survey Geologic Quadrangle Map GQ–439, scale 1:24,000.
Maldonado, Flovian, 1985, Geologic map of the Jackass Flats area, Nye County, Nevada: U.S. Geological Survey Miscellaneous Investigations Series Map I–1519, scale 1:48,000.
McCafferty, A.E., and Grauch, V.J.S., 1997, Aeromagnetic and gravity maps of the southwestern Nevada volcanic field, Nevada and California: U.S. Geological Survey Geophysical Investigations Map GP–1015, scale 1:250,000.
Moyer, T.C., and Geslin, J.K., 1995, Lithostratigraphy of the Calico Hills Formation and the Prow Pass Tuff (Crater Flat Group) at Yucca Mountain, Nevada: U.S. Geological Survey Open-File Report 94–460, 59 p.
Moyer, T.C., Geslin, J.K., and Flint, L.E., 1996, Stratigraphic relations and hydrologic properties of the Paintbrush Tuff nonwelded (Ptn) hydrologic unit, Yucca Mountain, Nevada: U.S. Geological Survey Open-File Report 95–397, 151 p.
Ponce, D.A., 1996, Interpretive geophysical fault map across the central block of Yucca Mountain, Nevada: U.S. Geological Survey Open-File Report 96–285, 13 p., 4 pl.
Potter, C.J., Dickerson, R.P., and Day, W.C., 1999, Nature and continuity of the Sundance fault, Yucca Mountain, Nevada: U.S. Geological Survey Open-File Report 98–266, 3 pl., scale 1:2,400, 16-p. pamphlet.
Potter, C.J., Dickerson, R.P., Sweetkind, D.S., Drake II, R.M., Taylor, E.M., Fridrich, C.J., San Juan, C.A., and Day, W.C., 2002, Geologic map of the Yucca Mountain region: U.S. Geological Survey Geologic Investigations Series I–2755, scale 1:50,000, 37-p. pamphlet.
Sawyer, D.A., Fleck, R.J., Lanphere, M.A., Warren, R.G., Broxton, D.E., and Hudson, M.R., 1994, Episodic caldera volcanism in the Miocene southwestern Nevada volcanic field—Revised stratigraphic framework, $^{40}Ar/^{39}Ar$ geochronology, and implications for magmatism and extension: Geological Society of America Bulletin, v. 106, p. 1304–1318.
Scott, R.B., 1992, Preliminary geologic map of southern Yucca Mountain, Nye County, Nevada: U.S. Geological Survey Open-File Report 92–266, scale 1:12,000.
Scott, R.B., and Bonk, Jerry, 1984, Preliminary geologic map of Yucca Mountain, Nye County, Nevada, with geologic sections: U.S. Geological Survey Open-File Report 84–494, scale 1:12,000, 9-p. pamphlet.

Scott, R.B., and Castellanos, M., 1984, Stratigraphic and structural relations of volcanic rocks in drill holes USW GU-3 and USW G-3, Yucca Mountain, Nevada: U.S. Geological Survey Open-File Report 84–491, 121 p., 1 pl.

Sibson, R.H., 1986, Brecciation processes in fault zones—Inferences from earthquake rupturing: Pure and Applied Geophysics, v. 124, p. 159–175.

Simonds, F.W., Whitney, J.W., Fox, K.F., Ramelli, A.R., Yount, J.C., Carr, M.D., Menges, C.M., Dickerson, R.P., and Scott, R.B., 1995, Map showing fault activity in the Yucca Mountain area, Nye County, Nevada: U.S. Geological Survey Miscellaneous Investigations Series I–2520, scale 1:24,000.

Spengler, R.W., Braun, C.A., Linden, R.M., Martin, L.G., Ross-Brown, D.M., and Blackburn, R.L., 1993, Structural character of the Ghost Dance fault, Yucca Mountain, Nevada, *in* High-level radioactive waste management—Proceedings of the Fourth International Conference, Las Vegas, Nev., April 26–30, 1993: LaGrange, Ill., American Nuclear Society, v. 1, p. 653–659.

Stewart, J.H., 1988, Tectonics of the Walker Lane belt, western Great Basin—Mesozoic and Cenozoic deformation in a zone of shear, *in* Ernst, W.G., ed., Metamorphism and crustal evolution of the western United States, Ruby volume VII: Englewood Cliffs, N.J., Prentice Hall, p. 683–713.

Sylvester, A.G., and Smith, R.R., 1976, Tectonic transpression and basement-controlled deformation in San Andreas fault zone, Salton trough, California: American Association of Petroleum Geologists Bulletin, v. 60, no. 12, p. 2081–2102.

Wahl, R.R., Sawyer, D.A., Minor, S.A., Carr, M.D., Cole, J.C., Swadley, W C, Laczniak, R.J., Warren, R.G., Green, K.S., and Engle, C.M., 1997, Digital geologic map of the Nevada Test Site area, Nevada: U.S. Geological Survey Open-File Report 97–140, scale 1:120,000.

Table 1. Borehole designations used on the geologic map of south-central Yucca Mountain, Nye County, Nevada.

Full name of borehole	Borehole designation used in this report
USW G-3	G-3
USW GU-3	GU-3
USW UZ-13	UZ-13
UE-25 WT#17	WT#17
USW WT-1	WT-1
USW WT-10	WT-10

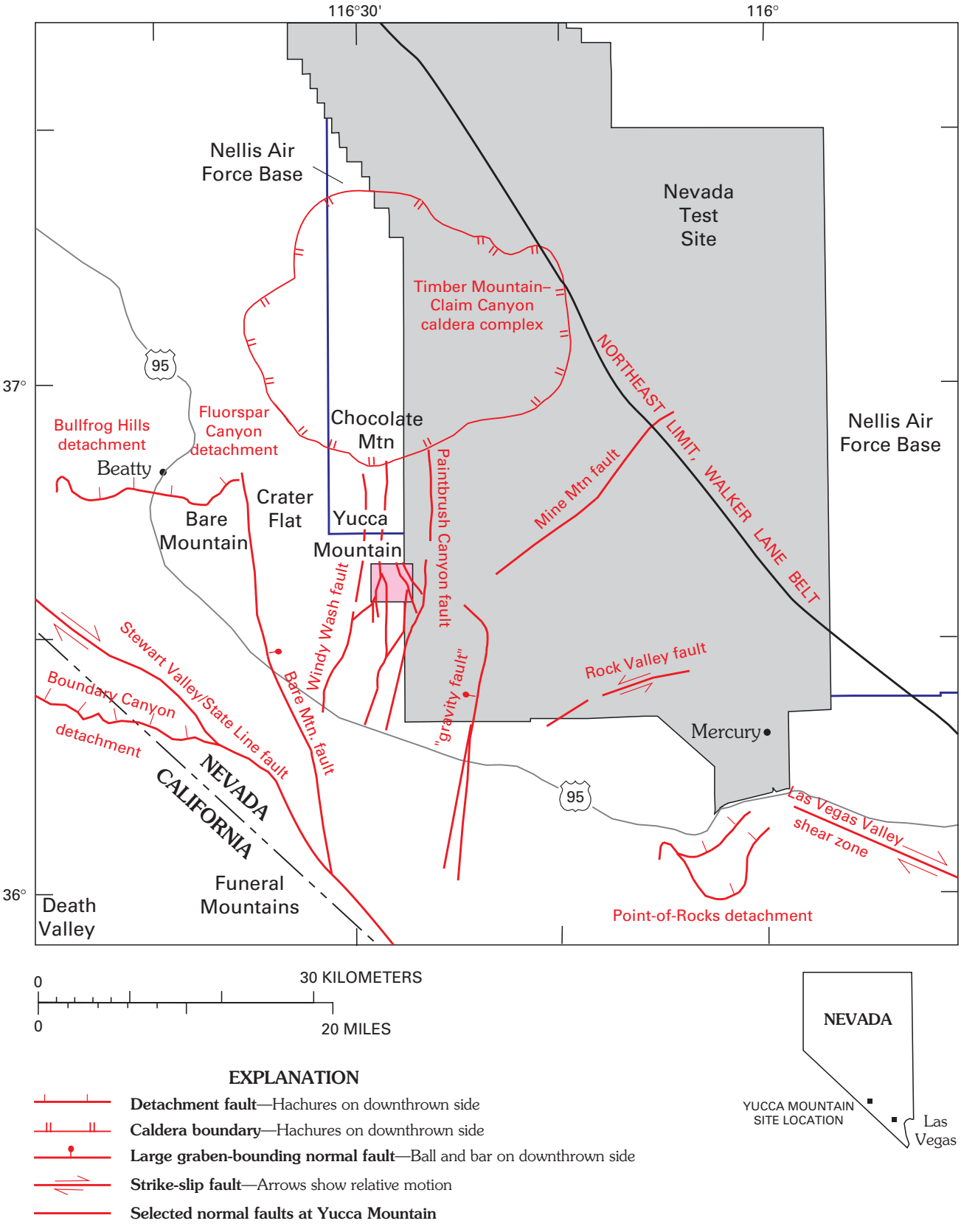

Figure 1. Location of map area (pink) and selected Neogene geologic features in the surrounding area, Nevada and California. Caldera boundary modified from Sawyer and others (1994, fig. 1, p. 1306). Location of detachment faults modified from Hamilton (1988). Location of Walker Lane belt boundary from Stewart (1988).

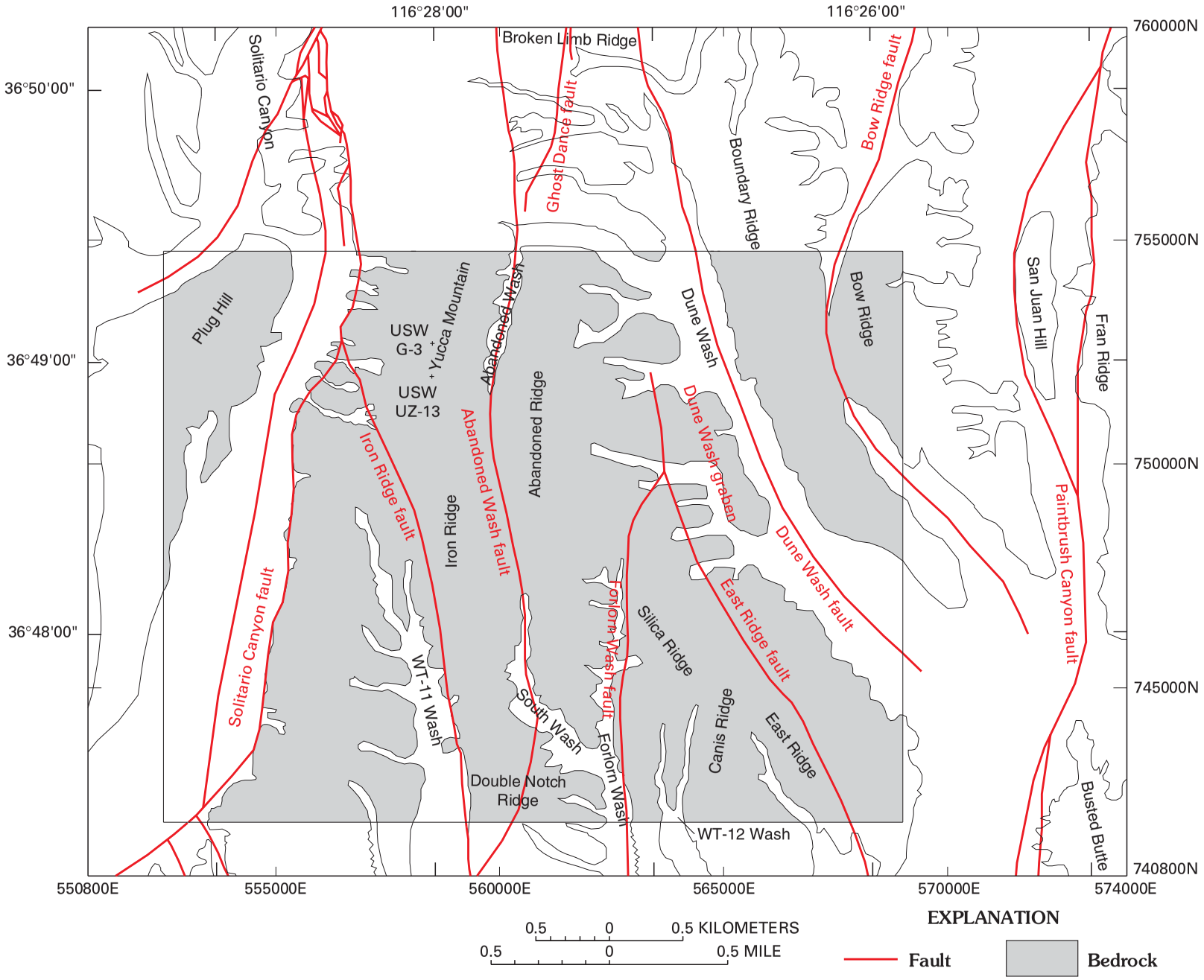

Figure 2. Location of prominent physiographic features in map area (inset), south-central Yucca Mountain, Nye County, Nevada.

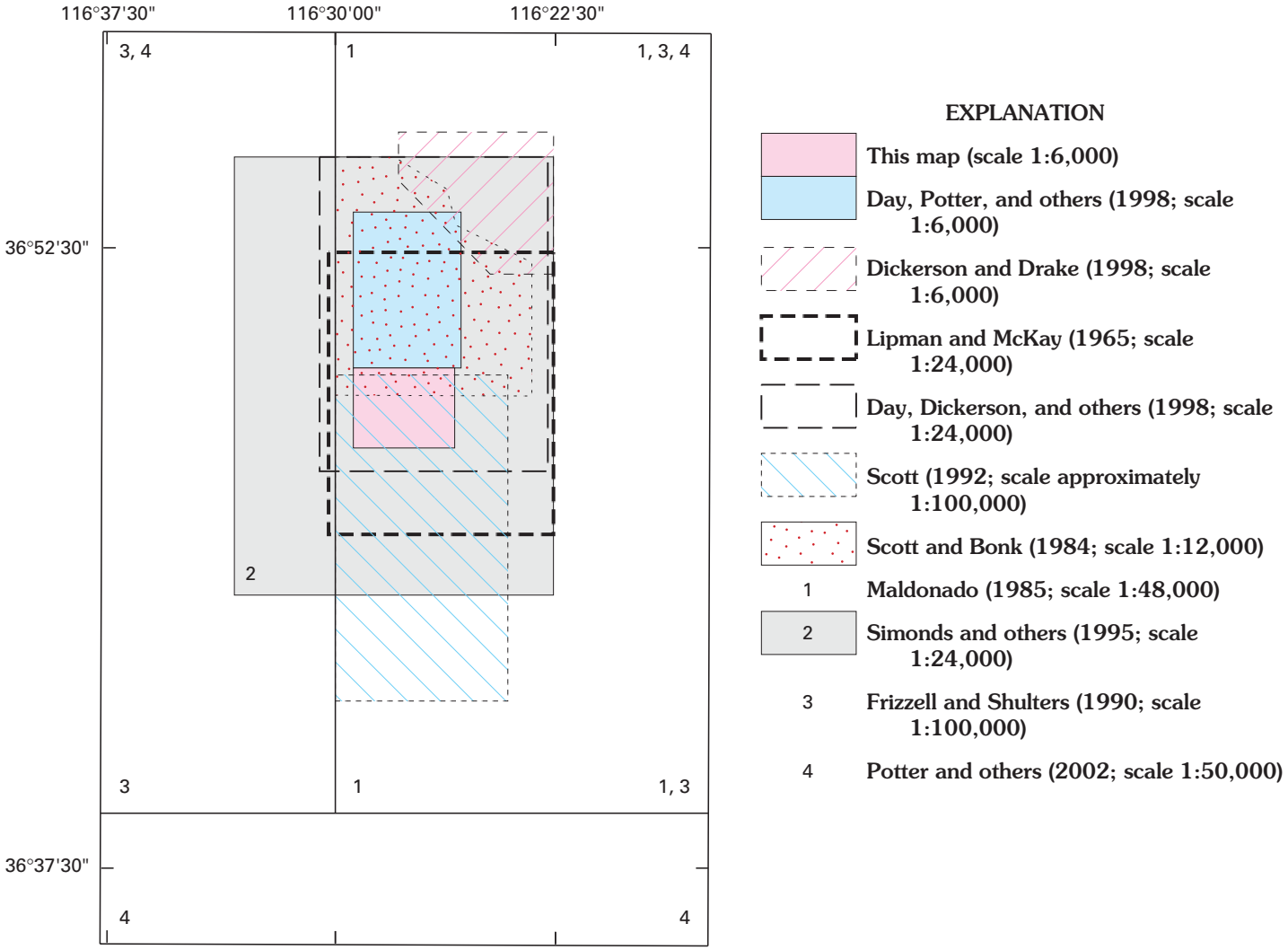

Figure 3. Index map showing location of map area relative to that of previously published maps, Yucca Mountain, Nevada.

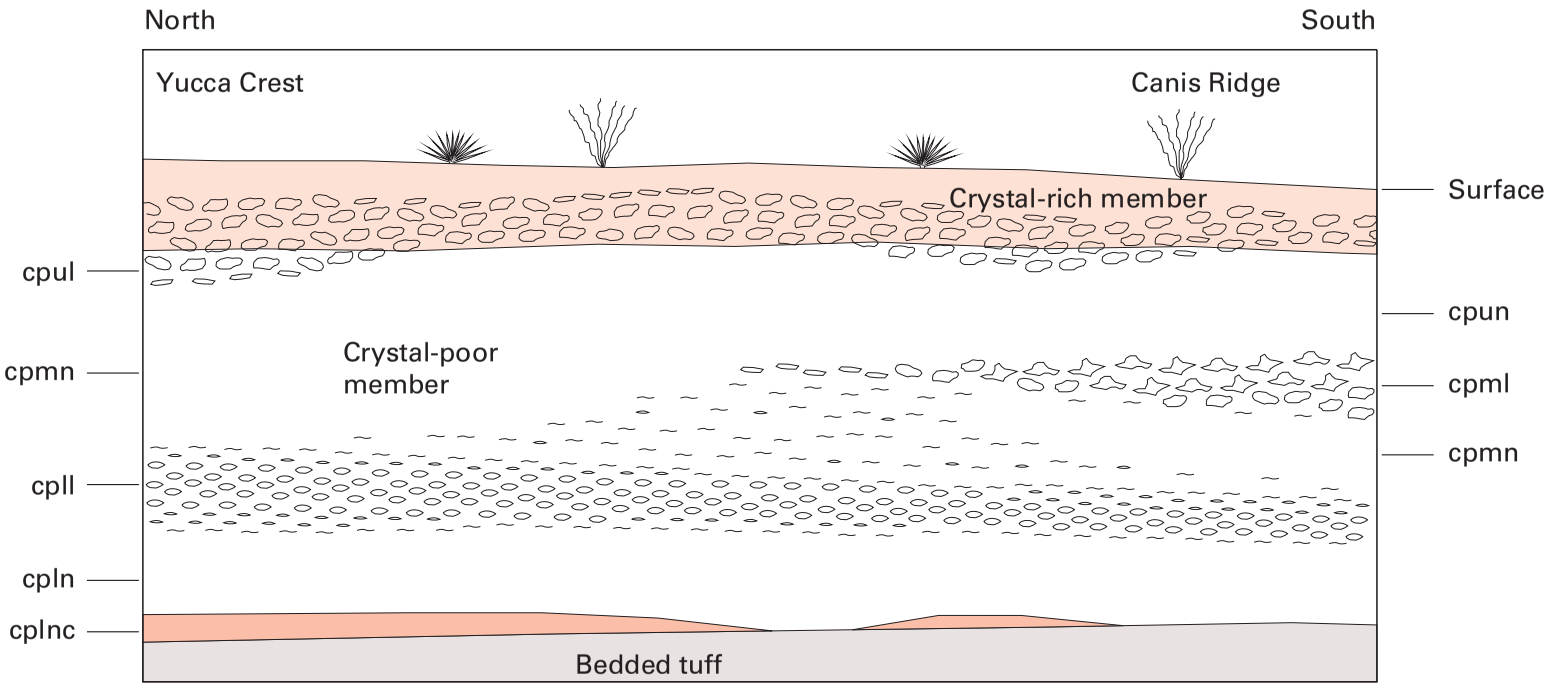

Figure 4. Lateral variation of zones within crystal-rich and crystal-poor members of the Tiva Canyon Tuff, Yucca Mountain, Nevada. cpul, **upper lithophysal zone;** cpun, **upper nonlithophysal zone;** cpml, **middle lithophysal zone;** cpmn, **middle nonlithophysal zone;** cpll, **lower lithophysal zone;** cpln, **lower nonlithophysal zone;** cplnc, **lower nonlithophysal zone, columnar subzone. Open circles represent lithophysae; wiggly lines represent vapor-phase partings.**

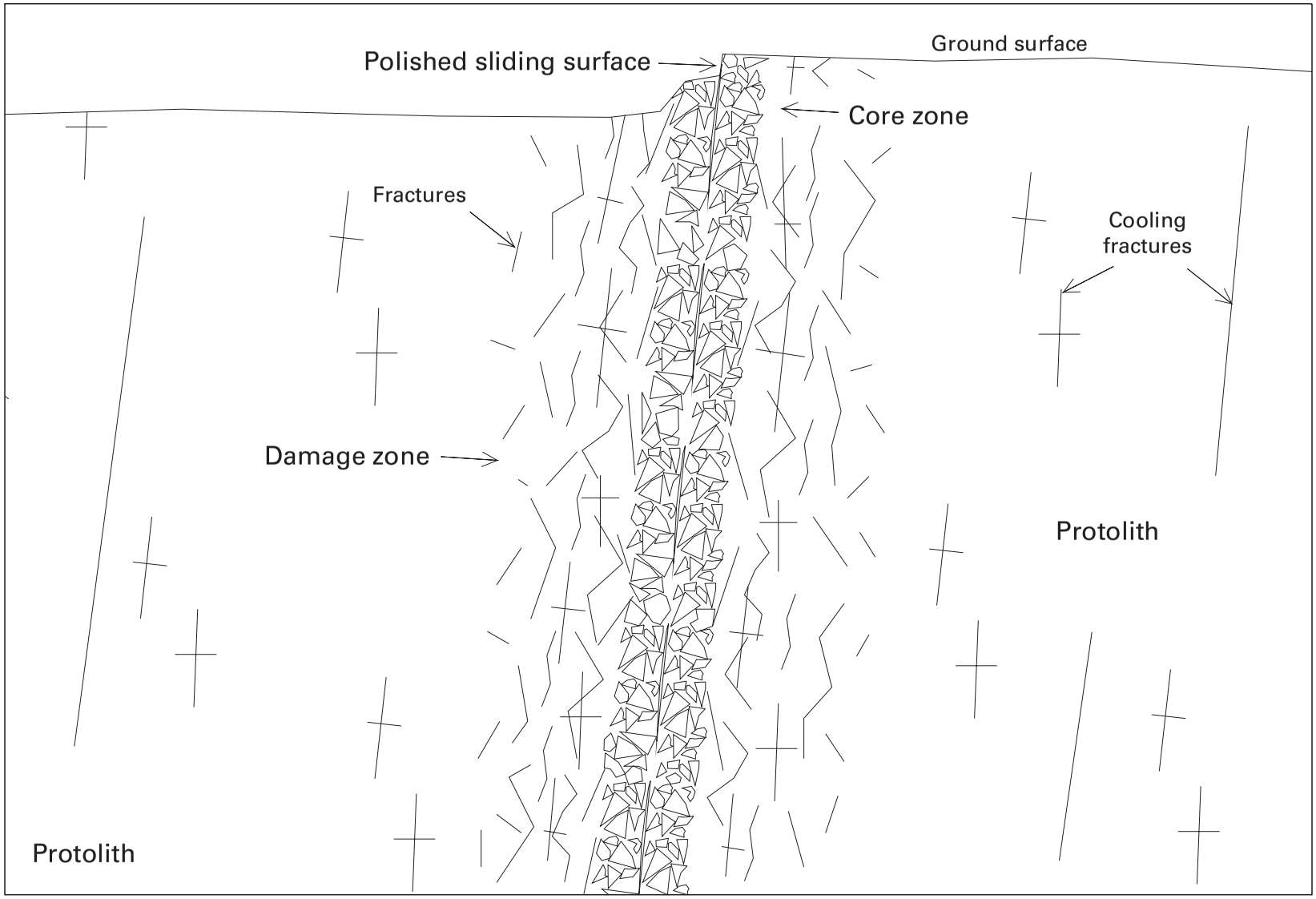

Figure 5. Terms related to fault zones. Welded tuffs typically exhibit cooling fractures unrelated to faulting. Scale varies with fault type. Not all faults contain all elements illustrated here.